

Low-cost methodology for the characterization of floc size in low turbidity and low alkalinity waters using image analysis

González-Galvis Juan Pablo ^{a,*}, Jaramillo Londoño Angela Maria ^b and Martínez Urrego Andres Felipe ^b

^a Faculty of Civil Engineering, Universidad Santo Tomás, Tunja 150001, Colombia

^b Faculty of Environmental Engineering, Universidad Santo Tomás, Bogotá 110231, Colombia

*Corresponding author. E-mail: juan.gonzalezga@usantoto.edu.co

 G-GJP, 0000-0002-3647-190X; JLAM, 0000-0001-9465-8513; MUAF, 0000-0002-6397-924X

ABSTRACT

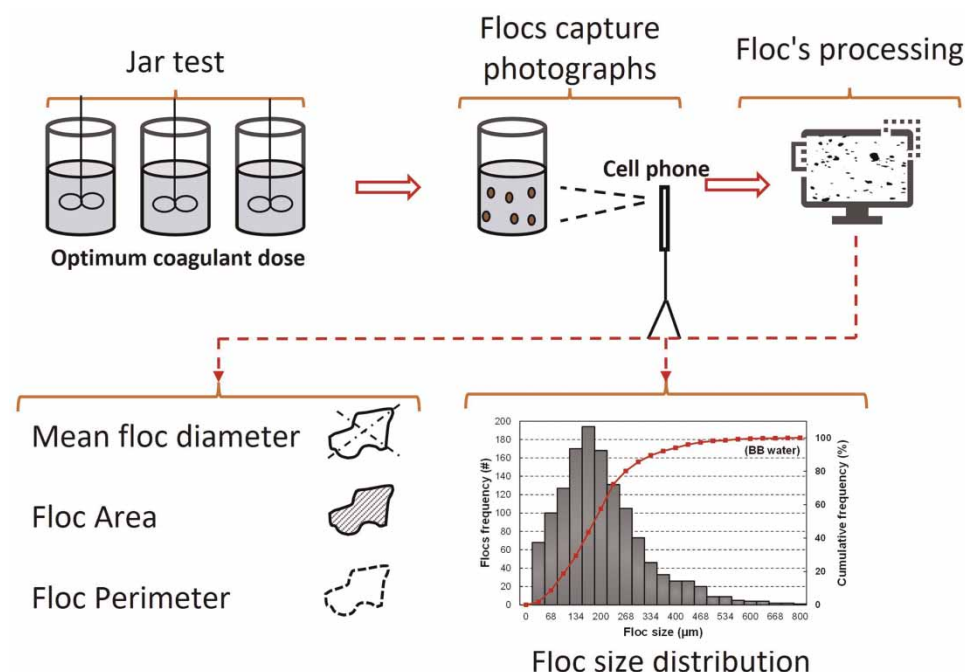
Floc-particle size in drinking water treatment is an important parameter for designing and operating clarification and filtration units. However, advanced techniques for floc characterization are not affordable in drinking water utilities in developing countries because they are expensive and require qualified and training personnel. Therefore, the main objective of this research was to develop and test a nonintrusive low-cost methodology for floc size characterization using a regular HUAWEI P30 cell phone equipped with 40 megapixels camera, which is significantly less expensive than a sophisticated high-speed high-resolution camera used for floc characterization based on image analysis. This technique does not require sample processing, which keeps unaltered floc/particles aggregates for analysis. The methodology was calibrated using four different source waters with low turbidity ($\leq 5.95 \pm 0.48$ NTU) and relatively low alkalinity ($\leq 52.4 \pm 4.12$ as CaCO_3), which are typical from the Andina Region in Colombia. This methodology demonstrated to be useful for obtaining the mean floc size (based on average Feret diameter), floc area, floc perimeter and circularity of aggregates formed by the addition of alum $[\text{Al}_2(\text{SO}_4)_3 \cdot 18\text{H}_2\text{O}]$ after 15 minutes of flocculation in a regular jar tester. The methodology also proved to be valuable for measuring floc sizes in a range between 33 μm and 1,200 μm .

Key words: coagulation, flocculation, flocs, image analysis, sedimentation

HIGHLIGHTS

- Development of a low-cost methodology for flocs size characterization in developing countries.
- Determination of floc physical characteristics, mean diameter, perimeter, area, and circularity.
- Impact of raw water turbidity and coagulant dose on flocs size.
- Calculation of the floc settling velocity in sedimentation units.

GRAPHICAL ABSTRACT



INTRODUCTION

In Colombia, many drinking water treatment plants (WTPs) work with multistage filtration units (MEF) (i.e., rapid filtration plus slow sand filtration) and disinfection processes for obtaining potable water. This combination of water treatments is also used by many countries worldwide (El-Taweel & Gamila 1999; Dastanaie *et al.* 2007). MEF plants in Colombia were designed and built to work without pre-treatment steps such as coagulation, flocculation, and clarification (sedimentation) processes, which make these facilities susceptible to unexpected water quality changes as a result of increasing turbidity concentrations. Since 2010, Colombia has experienced a strong weather oscillation, which is characterized by a prolonged period of wet weather known as El Niño and a dry and cold phase on an extended period of rain known as La Niña (Hoyos *et al.* 2013). The phenomenon of El Niño has profound effect on intensity of precipitation, river flow, and soil moisture in the Andina zone of Colombia (Poveda & Mesa 1996; Poveda *et al.* 2001). In contrast, the phenomenon of La Niña is characterized by intense and abundant rainfall and an increased river flow (Poveda & Mesa 1996; Mesa *et al.* 1997). Therefore, WTPs in Colombia must handle unexpected precipitation events throughout the year, which increase turbidity, solids concentration, and natural organic matter (NOM) concentrations in surface waters.

A water quality report from the National Health Institute of Colombia (INS 2019) showed that 88% of the municipalities in the Department of Boyacá, Colombia, located in the Andina region, which is the study area of this research, do not meet the drinking water quality standards. The presence of pathogenic organisms and turbidity concentrations higher than 2.0 NTU found in tap water are two of the crucial issues in these WTPs. Therefore, to meet the basic drinking water standards and mitigate climate change impacts, these WTPs should update their old systems by incorporating coagulation, flocculation, and clarification units. However, one drawback in the design of clarification units in developing countries is the lack of information on key design parameters such as floc size and structure (Jarvis *et al.* 2006). Some studies have found that particle number and particle size distribution (PSD) are two useful parameters in the selection of drinking water treatment process (Kavanaugh *et al.* 1980; Dempsey & O'Melia 1984).

Other studies suggest that turbidity may not be chosen as the best parameter for evaluation of process effectiveness, instead, particle number and PSD should be used to understand and control the removal of contaminants (Lawrence & Zimmermann 1976; Hunsinger *et al.* 1980). The study of floc size not only allows to improve the clarification process design, but also to assess the real impact of floc/particles characteristics on MEF units' performance (Gregory 1998; MWH 2012). To conduct floc size and particle characterization, different techniques

have been developed, which include light microscopy (Aguilar *et al.* 2003), electron microscopy (Movrocordatos *et al.* 2004), dynamic particle analysis (DPA) (McCurdy *et al.* 2004; González-Galvis & Narbaitz 2020a), high-performance size exclusion chromatography (HPSEC) method (Feride *et al.* 2019), and flocs zeta potential analysis (Zafisah *et al.* 2020). However, the main disadvantage of these techniques is that they require qualified and trained personnel as well as sophisticated and expensive equipment, which make them cost-prohibitive for developing countries.

In recent years, digital imaging analysis (DIA) has been improved and implemented for floc characterization (Wang & Gregory 2002; Sun *et al.* 2016). This method is simpler and more economic than others because it uses basic tools such as a photographic camera and a free computer program for processing the floc images obtained. Some advantages of this image analysis include: (1) Allowing quick measurement of the number of flocs; (2) Monitoring unaltered flocs by capturing images, in a mixed suspension while focusing on a plane at close distance (0.3–1.0 cm), in which the camera distance is measured from the tank wall that contain the suspension (Chakraborti *et al.* 2000); (3) Capturing floc size images using a regular jar testing apparatus, which is an economic and common tool in water treatment facilities (Chakraborti *et al.* 2000; Juntunen *et al.* 2014; Wang *et al.* 2014; Sun *et al.* 2016). Due to developing countries finding the cost prohibitive for the equipment's and the qualified personnel required for conducting floc size characterization, the main objective of this research was to develop and test a nonintrusive low-cost methodology for floc size characterization using a regular HUAWEI P30 cell phone equipped with 40 megapixels camera, which is significantly less expensive than a sophisticated high-speed high-resolution camera used for floc size characterization based on image analysis (Sun *et al.* 2016) and a regular jar test apparatus. Four different natural surface waters were used in the experiments as a calibration method and for comparison purposes. The floc size characterization reported in this study included floc size (based on average Feret diameter) (Benjamin & Laurer 2013), floc area, floc perimeter, floc circularity, and floc size distribution of each water tested.

MATERIALS AND METHODS

Water tested

The experiments were conducted using different raw surface water samples collected at the intake of four WTPs located in the Department of Boyacá, Colombia, which are currently treated with MEF units: (1) in the town of Boyacá (BB water); (2) in the town of Soracá (SR water); (3) in the town of Ventaquemada (VQ water) and (4) in the town of Turmequé (TM water). These locations were chosen for logistic reasons and because all are low turbidity and alkalinity waters. Water samples were collected at different times of the year in 2021 and were stored at $(4 \pm 1\text{ }^{\circ}\text{C})$ until testing to avoid solids' and organics' degradation inside the buckets.

Jar test experiments

Conventional gravity settling (CGS) experiments were conducted using a regular jar test apparatus with six 2 L round beakers (F6300 EQ Equipment, Colombia). All the coagulation, flocculation and conventional gravity settling (C/F/CGS) jar tests were conducted with the following protocol: (1) rapid mix at 100 rpm ($G=368\text{ s}^{-1}$) for 1 min; (2) slow mixing at 40 rpm ($G=93\text{ s}^{-1}$) for 15 min and (3) sedimentation for 30 min. This protocol is recommended for conducting C/F/CGS jar tests (Kawamura 2000; AWWA 2011). The C/F/CGS experiments were performed using six different alum doses (i.e., 10, 20, 30, 40, 50, and 60 mg/L as Al_2O_3). After the CGS experiments, settled water turbidity was measured immediately and settled water samples were collected for further analyses of apparent color, and pH using standard methods for the examination of water (APHA 2017). The C/F/CGS experiments were duplicated, and the results are based on the arithmetic average and the standard deviation was used as experimental error between the two test.

Floc size measurement

Floc sizes obtained after coagulation and 15 minutes of flocculation in the jar test were measured and quantified using a digital image analysis (DIA) system. In the following minute after flocculation time, the mixing speed was lowered from 40 rpm to the minimum speed of 10 rpm in the jar tester apparatus. The intent was to allow a reduction in the circulation speed of the flocs inside the jar. Flocs were captured following a nonintrusive digital imagery process improved by Sun *et al.* (2016). The setup used in this research for DIA included a HUAWEI P30 cell phone equipped with a 40 Mega Pixels Super Spectrum camera with a focal aperture of 1-to-2.8 ($f/1.8$), a 2 L round glass beaker, and an adjustable tripod with a cell phone base (Figure 1). The jar test apparatus base light

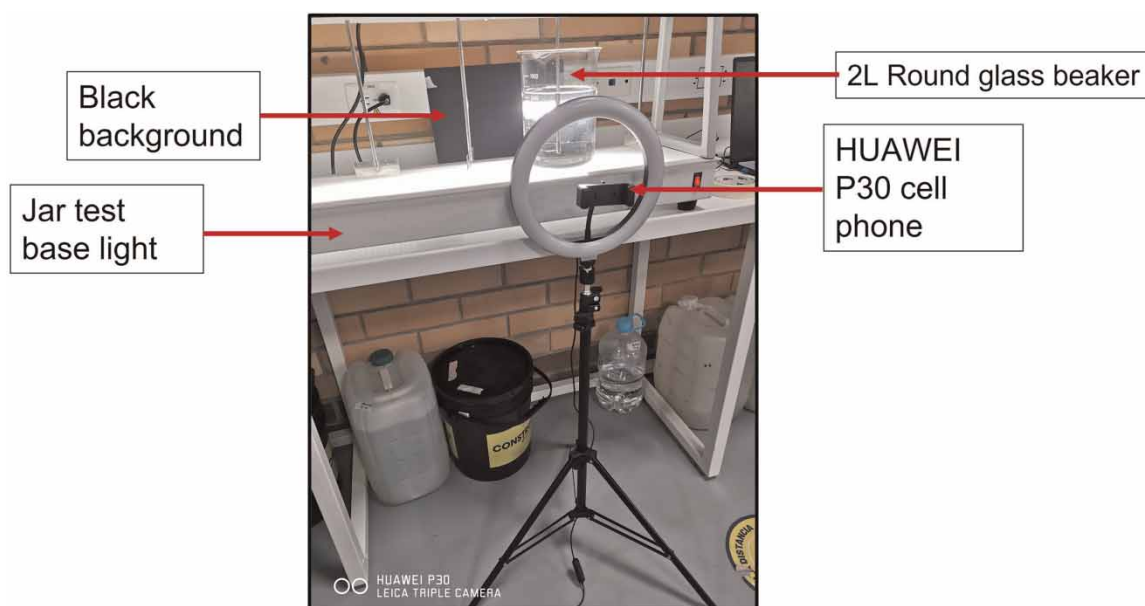


Figure 1 | Floc size measurements experimental setup.

was used as a source to illuminate the flocs inside the jar. To keep the cell phone camera completely static and avoid blurring of the floc's images, the camera was triggered by using a Bluetooth remote shutter. The HUAWEI P30 camera was placed at a distance of 15 cm away from the jar wall. To improve the floc visualization, the camera was operated with an optical zoom of 5X and a black background was used. Before taking photographs of the flocs inside the jar, air bubbles attached to the jar wall were removed with a glass stirring rod to avoid adding noise and interference in the DIA. The cell phone camera was set up as follow: (1) picture type (professional); (2) light sensitivity (ISO-200); (3) obturation speed (S 1/100); (4) autofocus (AF) continuous (C), for moving objects. The floc pictures were processed using ImageJ computer program (National Institutes of Health, Bethesda, MD). The floc size measurement experiments were conducted three times at room temperature ($\sim 20 \pm 2$ °C) using BB water to test the method and assess reproducibility. In each test, the diameter of approximately 1,300 flocs were measured. An example of flocs images captured inside of the jar using the proposed set-up and the ImageJ computer program settings, are shown in Figure 2(a) and 2(b), respectively.

Floc identification and image analysis

Floc size found in WTPs after coagulation and flocculation processes may be affected by several factors such as: (1) concentration, origin, and composition of the natural organic matter (NOM); (2) alkalinity, temperature, pH and hardness of raw water; (3) coagulant type and dose; and (4) coagulation and flocculation mixing intensity (i.e., velocity gradient, $G\text{-s}^{-1}$) (Edzwald & Haarhoff 2012; González-Galvis & Narbaitz 2020a). In this research the floc size measurements followed the optimum coagulant dose of each water with the same flocculation mixing intensity for all water tested at 40 rpm (93 s^{-1}). Once the flocs' pictures had been obtained (Figure 2(a)), the steps shown in the Figure 3, were followed to set-up the ImageJ computer program and identify flocs as black points and measure them (Figure 2(b)). To establish the reference scale in the photograph by the ImageJ computer program (i.e., set-scale step 6 Figure 3), a stainless-steel caliper with an opening of 1.0 millimeter was placed in the jar wall at a distance of 15 cm from the cell phone camera. The total time to obtain a floc size characterization with a single picture is approximately between 50 and 60 minutes. That time includes 16 minutes for the jar test (1 minute coagulation plus 15 minutes flocculation), 1 minute for taking at least five pictures, and approximately 30–40 minutes for analyzing the best picture with the ImageJ computer program (Figure 3).

Analytical methods

The pH of all the water samples was measured using a HANNA HI9125 pH meter (Bogotá, Colombia). Turbidity was determined using a Lovibond® TB210 turbidimeter (Sarasota, FL). Before measuring the samples, the nephelometric turbidity meter was calibrated with the 0.1 NTU and 20 NTU standards supplied by Lovibond®. The minimum turbidity value measured was 0.1 NTU. According to the turbidity meter's manual, the repeatability

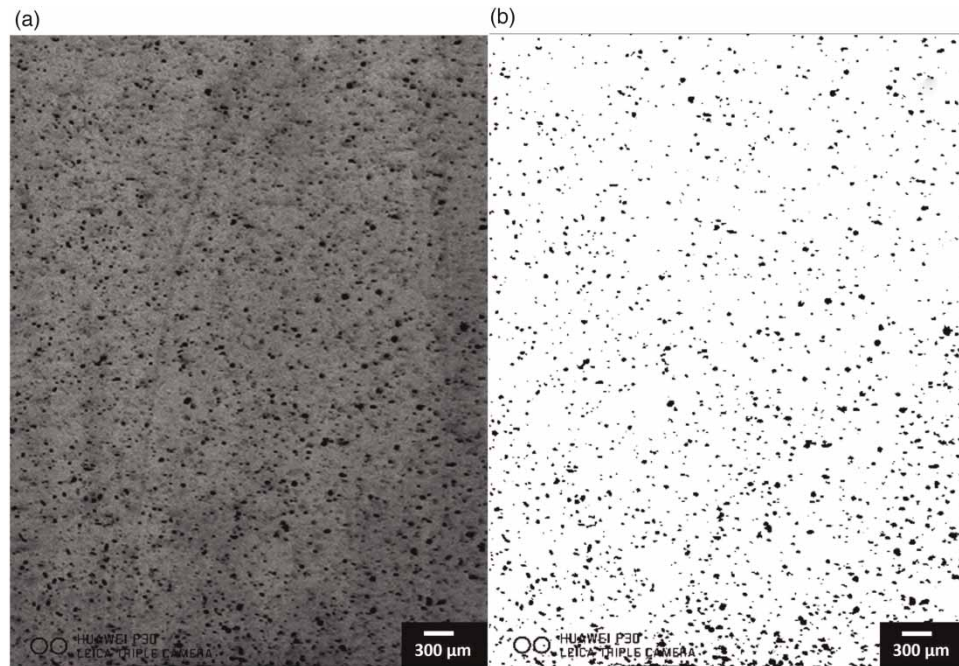


Figure 2 | Image treatment to determine the floc size in the jar test treating BB water: (a) conversion to grayscale and 8-bit image; (b) ImageJ computer program setting steps to highlight flocs as black points for analysis.

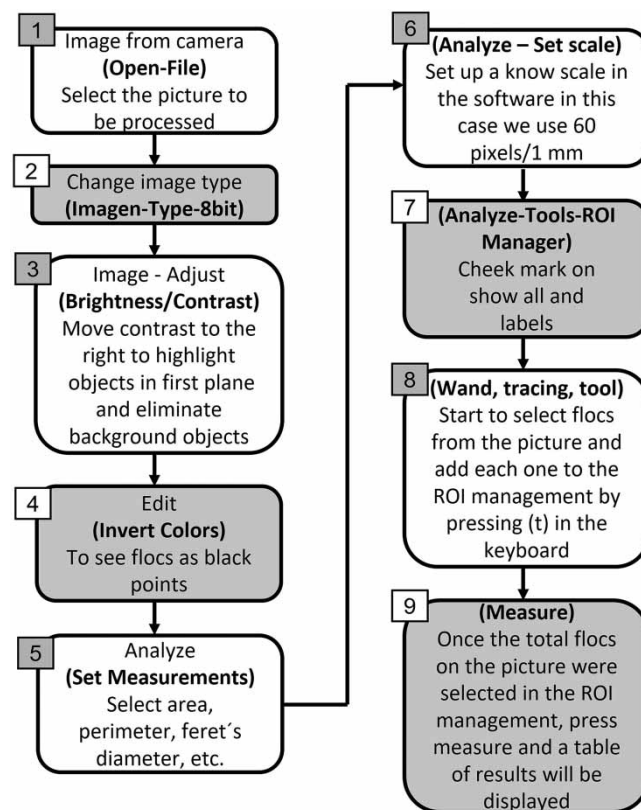


Figure 3 | Flow chart of floc identification and image analysis.

(or precision) of the measurements is $\pm 1\%$ or ± 0.01 NTU, whichever is greater. The total hardness and alkalinity of the raw water were determined according to standard methods 8226 (2340) and 2320, respectively (APHA 2017). Apparent colour was measured using a Spectroquant[®] move 100 Merck KGaA (Darmstadt, Germany).

RESULTS AND DISCUSSION

Water quality

Table 1 shows the characterization of four different raw waters (i.e., BB, SR, VQ, and TM) collected for this research in different periods of 2021. In general, the composition for all waters describes low turbidity, low alkalinity, and low hardness characteristics. SR and VQ waters were collected in raining season in which they have their maximum peak of turbidity and yellowish color, whereas BB and TM waters were collected in a dry period were quite transparent. The low apparent color of BB and TM waters is consistent with the low turbidity values registered for each one (1.67 and 0.53 NTU, respectively). The historic record of the raw water quality from the last five years showed that the maximum turbidity values of BB and TM waters were below 3.0 and 2.0 NTU, respectively even in a raining season. The relatively high apparent color found in SR and VQ waters, could be linked to an important concentration of NOM (humic and fulvic acids), which impart color to the water (Edzwald & Haarhoff 2012; Sillanpää *et al.* 2018), as well as the possible presence of inorganic compounds such as iron and manganese (MWH 2012). Compounds contributing to the yellowish color in water are generally collected from contact with decaying vegetation, and runoff of dissolved iron (Constantine 1982). A water quality report from 2019 and 2020 provided by the public service office of Soracá, Boyacá, showed an iron concentrations of 0.35 mgFe/L in the raw water, which contributes to its high yellowish appearance (Table 1). In contrast, BB and TM raw waters are noticeably clear with turbidities between 1.67 and 0.53 NTU, respectively. The low turbidity concentration and the low apparent color of these two waters (i.e., BB and TM) is the result of raw pristine water (i.e., fresh and clean water), coming from a nearby mountain, which is low in NOM and other inorganic compounds that negatively impact its physical characteristics, even in a raining period the maximum turbidity values registered for this water are below 3.0 NTU.

Table 1 | Raw water characterization

Parameter	BB (March 2021)	SR (April 2021)	VQ (June 2021)	TM (June 2021)
pH	6.79 ± 0.02	7.18 ± 0.11	6.57 ± 0.02	7.26 ± 0.08
Turbidity (NTU)	1.67 ± 0.11	5.95 ± 0.48	2.27 ± 0.14	0.53 ± 0.02
Alkalinity (mg L ⁻¹ as CaCO ₃)	25 ± 4.08	52.4 ± 4.12	10 ± 1.6	12 ± 1.63
Apparent Color (Pt-Co)	33.5 ± 4.31	81.3 ± 4.78	57 ± 3.7	3.0 ± 1.41
Total Hardness (mg L ⁻¹)	24.7 ± 1.9	54.3 ± 7.9	11 ± 1.9	16.3 ± 1.2

Values are average ± one standard deviation (*n*=3).

Selection of coagulant doses

Figure 4 shows the change in turbidity removal and target pH for different alum concentrations of the water samples. Low turbidities and NOM concentrations in water after coagulation, flocculation, and sedimentation (C/F/SED) processes are the result of particle destabilization, which can be attributed to charge neutralization followed by sweep flocculation (Chakraborti *et al.* 2000). As shown in Figure 4, the target pH (red triangles) for BB, TM, and VQ water with a coagulant dose between 20 and 40 mg/L as Al₂O₃ was remarkably similar with values of 5.20 and 5.13, respectively. Meanwhile for SR water the target pH was 7.03. This high final pH observed in SR water after coagulation (i.e., dose of 20 mg/L as Al₂O₃) is related with its relatively high alkalinity (i.e., 52 mg L⁻¹ as CaCO₃) in comparison with the low alkalinity found in BB, TM, and SR waters (Naceradska *et al.* 2019). An interpretation of the pC-pH diagram of Amirtharajah & Mills 1989, suggests that the main particle removal mechanism for BB, VQ and TM water would be the charge neutralization, while for SR water the main particle removal mechanism would be sweep coagulation. The addition of coagulants to the water creates and adds new particles, which results in additional turbidity, and this may underestimate turbidity removals by sedimentation (SED) of low turbidity waters (Edzwald & Haarhoff 2012; González-Galvis & Narbaitz 2020b). The authors found that adding a coagulant dose of 20 mg/L as Al₂O₃ increases the raw water turbidity by 7.2% after 15 minutes of flocculation of BB water. Thus, herein the authors report the optimum coagulant dose for each water based on flocculated water turbidity removals instead of the raw water turbidity removals.

Flocculated turbidity removals of 34 and 47% after treating BB and TM water were obtained with an alum dose of 40 mg/L Al₂O₃ as shown in Figure 4(a) and 4(c), respectively. While flocculated turbidity removals of 80 and

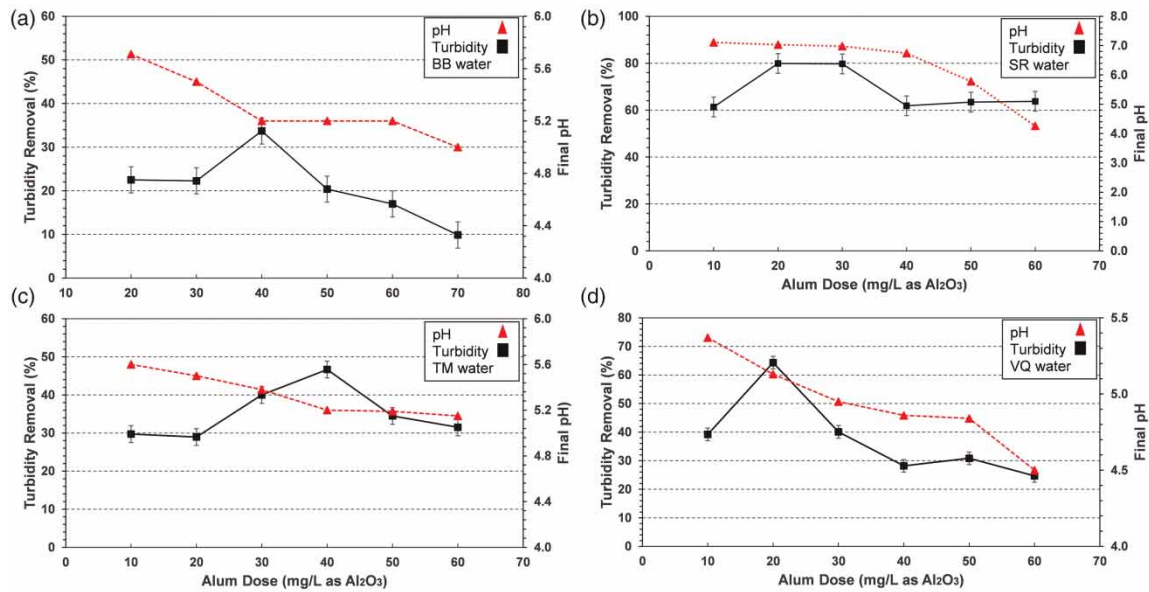


Figure 4 | Final pH and turbidity removal as a function of alum dose: (a) BB water, (b) SR water, (c) TM water, and (d) VQ water. (error bars indicate one standard deviation) ($n=2$).

64% were obtained treating SR and VQ water with a lower alum dose of 20 mg/L Al₂O₃ as shown in Figure 4(b) and 4(d). The low turbidity removals obtained by treating BB and TM water in comparison with SR and VQ water, are related with their low initial turbidities (i.e., 0.53 and 1.67 NTU), which require high coagulant doses to achieve particle destabilization and to obtain large and heavy flocs to settle.

Floc size measurement

Flocs size measurement reproducibility and accuracy

To evaluate the accuracy and reproducibility of the methodology proposed in this study to identified and measure flocs following the procedure described in Figure 3, three different jar tests were conducted for BB water. In each test a set of pictures were taken. The analysis and floc measurements were conducted on a single picture for each test. In each picture up to 1,330 flocs were identified and measured. Figure 5 shows the results of the flocs size distribution frequency (number based) obtained.

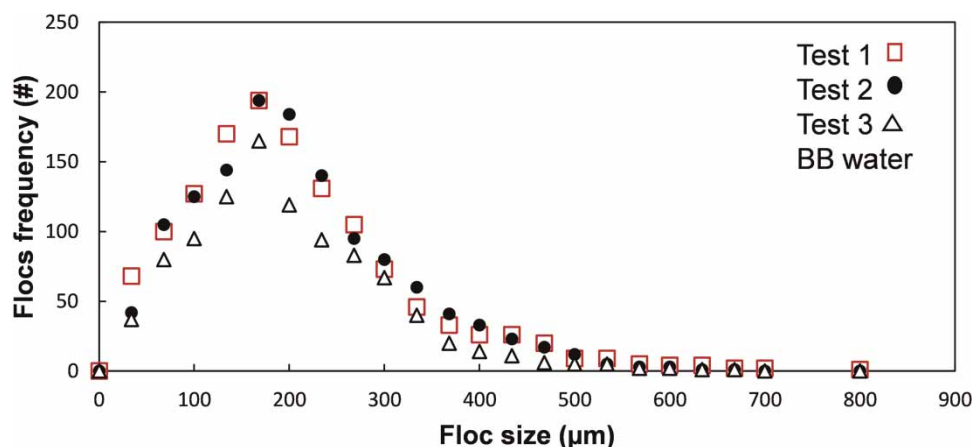


Figure 5 | Flocs size distribution obtained in three different test treating BB water. Conditions: Turbidity, 1.67 ± 0.11 NTU; Alkalinity 25 ± 4.08 as CaCO₃; Coagulant dose 40 mg/L as Al₂O₃ ($n=1330$) for each test.

According to Figure 5, there was a wide range of floc sizes (i.e., 31–400 μm) for 95% of the population and fewer sizes beyond this range for the rest of the flocs and the three different test showed fairly comparable results. In addition, there was a narrower range of maximum frequency (68–268 μm). The average mean floc size among

the three different tests was $197 \pm 100 \mu\text{m}$. One-way ANOVA ($\alpha=0.05$) of the floc size distribution (Figure 5), showed that the mean floc size obtained in all three different tests are statistically equal ($P\text{-value}=0.034$) and the confidence limits of the slope does not include zero. In addition, the floc sizes distribution found in the three different tests with BB water was similar as that reported by other studies using an image analysis measurement technique for alum floc characterization for floc ranging from 10 to $400 \mu\text{m}$ (Chakraborti *et al.* 2000) and between 20 and $300 \mu\text{m}$ (Gorczyca & Ganczarzyk 1999).

BB water floc size distribution

Once the methodology was tested for assessing its accuracy and reproducibility (Figure 5), a floc size test measurement for BB water was conducted. In this case a jar test was conducted in one beaker with the optimum alum dose found for this water (Figure 4(a)). Then, several pictures (i.e., 60 pictures in total) with the HUAWEI P30 cell phone camera were taken after 15 minutes of flocculation. To conduct the floc size analysis, one picture with the best observable floc size distribution was chosen. Like the floc size distribution shown in Figure 5, a similar wide sizes of flocs were found ($31\text{--}815 \mu\text{m}$) as shown in Figure 6. The mean floc size of this distribution was $198 \pm 110 \mu\text{m}$. Also, most flocs ($>80\%$) were smaller than $268 \mu\text{m}$, while the bigger flocs $400\text{--}815 \mu\text{m}$ represented just 5% of the population. As in this study the precision of the method was not assessed or compared with other techniques because they are not available in Colombia. It is recommended, when possible, to compare the proposed methodology with a conventional one (i.e., DPA, or light microscopy).

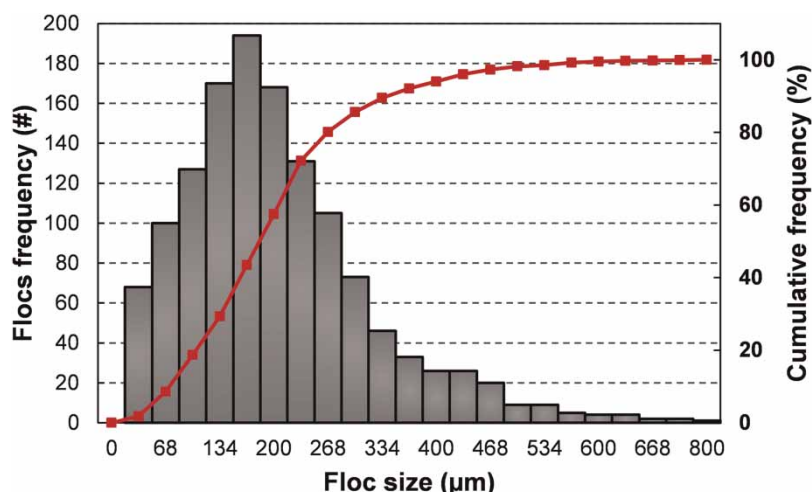


Figure 6 | Floc size distribution obtained in the treatment of BB water. Conditions: Turbidity, $1.67 \pm 0.11 \text{ NTU}$; Alkalinity $25 \pm 4.08 \text{ as CaCO}_3$; Coagulant dose $40 \text{ mg/L as Al}_2\text{O}_3$ ($n=1,354$).

Another important set of parameters obtained with the methodology proposed in this study were floc area and perimeter. The mean floc area and mean perimeter found in BB water was $33,500 \mu\text{m}^2$ and $710 \mu\text{m}$, respectively. Another two common parameters for floc size characterization are the shape factor and the sphericity. The shape factor is related to the particle surface area and to its volume, and the sphericity is defined as the ratio of the area of a sphere to the area of the particle under study (Benjamin & Laurer 2013). In this research the floc shape factor (circularity) was calculated directly by the software as a function of the longest axis divided by the longest length of a line perpendicular to that axis. Flocs in BB water had in average a shape factor of 0.8. This shape factor agrees with the floc shapes observed in Figure 2, which are close to an ideal circle. The floc sizes obtained in this study allowed the estimation of the floc settling velocity (FSV). In this case, the FSV of flocs from BB water is expected to be in the range of $0.072\text{--}5.45 \text{ m/h}$, with floc sizes between 31 and $268 \mu\text{m}$, respectively, which represents 80% of the total population. The FSV in BB water was calculated with the following assumptions: (a) water temperature of 10°C , which is the lowest and critical temperature of BB water in rainy season (i.e., make coagulation hydrolysis slow down) (Edzwald & Haarhoff 2012) and (b) floc density of 1.05 g/cm^3 , which is the density found in freshly precipitate hydroxides (Al, Fe, Mg) (Benjamin & Laurer 2013). The range of FSV found in the treatment of BB water is in between the settling velocities ($2\text{--}5.5 \text{ m/h}$) of a wide floc range (i.e., small fragile alum floc to large alum floc) as reported by water treatment plant design books (MHW 2012).

SR water floc size distribution

From a single picture of SR water, a total of 1,373 flocs were identified and measured. Figure 7 shows that the floc size found in SR water also had a wide size distribution in the range of 34–1,200 μm . In this water many flocs (>80%) were smaller than 400 μm . In contrast, the larger flocs (500–1,200 μm) only accounted for a small population (10%). The mean floc size of SR water was $277 \pm 160 \mu\text{m}$. SR water mean floc size was bigger than BB water ($197 \pm 100 \mu\text{m}$). This could be due to a better particle agglomeration as a result of the difference in the raw SR water turbidity ($5.95 \pm 0.48 \text{ NTU}$) versus BB raw water turbidity (1.67 ± 0.11). The mean floc area of $104,471 \mu\text{m}^2$ and mean perimeter of 1,204 μm of SR water were the highest values among the four different waters tested.

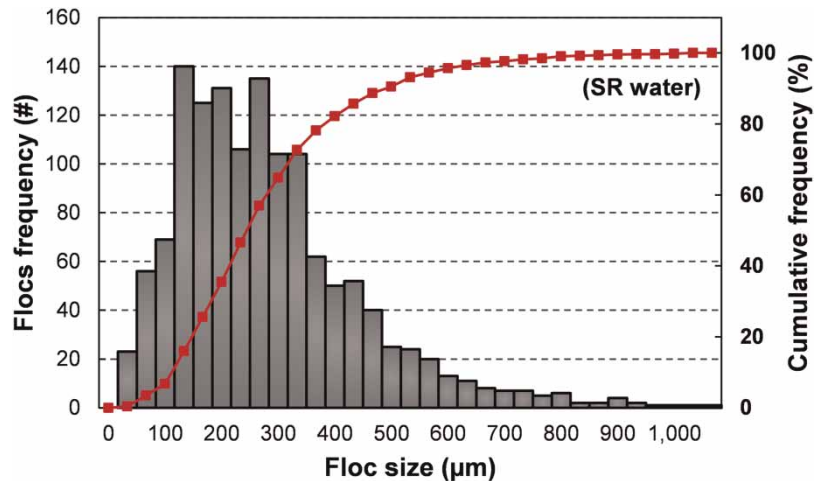


Figure 7 | Floc size distribution obtained in the treatment of SR water. Conditions: Turbidity, $5.95 \pm 0.48 \text{ NTU}$; Alkalinity 52.4 ± 4.12 as CaCO_3 ; Coagulant dose 20 mg/L as Al_2O_3 ($n=1373$).

Flocs in SR water had in average a shape factor of 0.7. This shape factor would mean that flocs formed while treating SR water were less round (i.e., a bit more like an ellipse in their shape than BB water). FSV in SR water was calculated with the same water temperature and floc density than those of BB water. FSV in SR water is expected to be in the range of 0.087–12.06 m/h, which is in between the FSV ranging from 2 to 5.5 m/h found in water treatment plant design books (MHW 2012).

VQ water floc size distribution

VQ water, characterized with an initial turbidity of $2.27 \pm 0.14 \text{ NTU}$ also showed a wide range of different floc sizes obtained with a single picture with a total of 1,390 flocs as shown in Figure 8. Floc size distribution in VQ water ranged from 33 to 662 μm with a mean diameter of $177 \pm 98 \mu\text{m}$. The floc size distribution of VQ water showed that 90% of the flocs were between 68 and 300 μm in size, while 1% were smaller than 68 μm and only 9% were bigger than 300 μm . A small percentage of flocs are flocs with diameter of 33 μm . Thus, the technique developed in this study does not allow to identify and measure flocs smaller than 33 μm . Therefore, to measure floc particle sizes lower than 33 μm , other techniques such as DPA, or laser diffraction analyzer must be used (Goula *et al.* 2008; González-Galvis & Narbaitz 2020b). In clarification processes (i.e., sedimentation and dissolved air flotation), it is expected to remove flocs and particles with diameters higher than approximately 13 μm , and the remaining flocs and particles (i.e., those with diameters less than 13 μm) are expected to be removed through filtration processes (González-Galvis & Narbaitz 2020b). Therefore, the proposed methodology can be used to know the mean floc size, the floc size distribution, the flocs' area and perimeter and the settling velocity, which could be useful for designing clarification units.

The mean floc area and perimeter found in VQ water were $40,062 \mu\text{m}^2$ and 745 μm , respectively. Flocs in VQ water had an average shape factor of 0.8. The FSV of a wide range (68–300 μm) found in VQ water is expected to be in the range of .34–6.79 m/h, which agrees with the range of 2–5.5 m/h reported in the literature (MHW 2012). Floc area, perimeter, and shape of flocs in water could help to understand particles' settling mechanisms in a

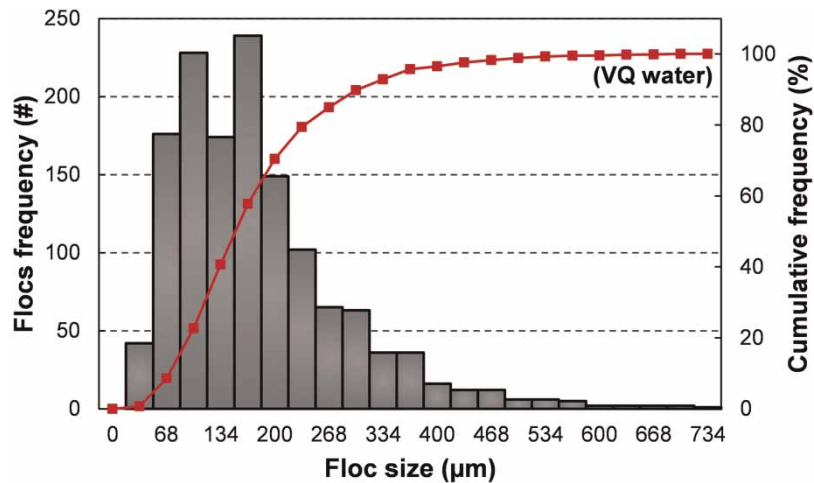


Figure 8 | Floc size distribution obtained from the treatment of VQ water. Conditions: Turbidity, 2.27 ± 0.14 NTU; Alkalinity 10 ± 1.6 as CaCO_3 ; Coagulant dose 20 mg/L as Al_2O_3 ($n=1389$).

sedimentation tank, as well as to identify flocs/particles/bubbles attached and removal mechanisms in dissolved air flotation (DAF) units and filtration units. Thus, additional studies should be conducted on this field to allow water treatment plant designers to have a better understanding of these mechanisms, which are usually explained theoretically (Edzwald 2010; MHW 2012; Benjamin & Laurer 2013).

TM water floc size distribution

TM water had the lowest raw water turbidity among the four waters tested (0.53 ± 0.02 NTU), and the lowest flocs/particles concentration. For TM water, a single picture identified and measured only 100 flocs, while for the other three waters (i.e., BB, SR and VQ), it captured more than 1,000 flocs. Nevertheless, it was still possible to obtain a wide floc size distribution as shown in Figure 9.

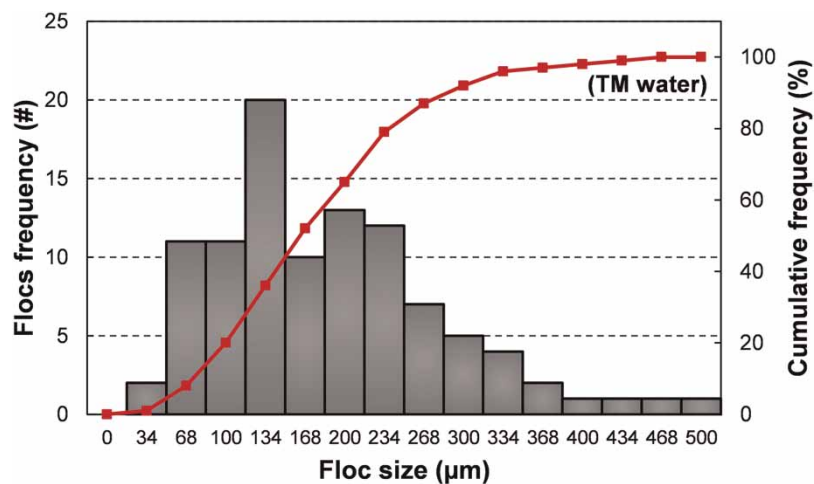


Figure 9 | Floc size distribution obtained in the treatment of TM water. Conditions: Turbidity, 0.53 ± 0.02 NTU; Alkalinity 12 ± 1.63 as CaCO_3 ; Coagulant dose 40 mg/L as Al_2O_3 ($n=100$).

The mean floc size obtained in TM water from the distribution showed in Figure 8 was 181 ± 88 μm . Most flocs (80%) fall in a size range of 68–234 μm , while a small percentage (20%) are outside of this range. In this water the mean floc area and the mean perimeter of the flocs were 43,430 μm^2 and 753 μm , respectively. The shape factor of flocs from TM water had different values from 0.5 (i.e., large ellipse flocs shape) to 1.0 (i.e., perfect circle flocs shape) with an average of 0.8.

Coagulant dose and raw water turbidity impact on floc area and perimeter

Although, the addition of coagulant increases the particles and the raw water turbidity, as well as the average flocs surface area and perimeter, it was observed that in the four waters tested the floc area and perimeter

were influenced by the raw water turbidity rather than the coagulant dose added as shown in Figure 10(a) and 10(b). The higher floc area and perimeter obtained for SR water suggest that the addition of an alum dose of 20 mg/L Al_2O_3 is sufficient to obtain big flocs that precipitate and sweep small flocs and particles from the water in a sedimentation unit, which is also known as sweep-flocculation mechanism (MHW 2012; Benjamin & Laurer 2013).

In general, the methodology for floc characterization developed and tested in this research permitted the measurement of a wide range of floc sizes distribution with a single picture for all the waters tested. However, a single picture does not allow the comparison of the data obtained in each water to assess the floc distribution and concentration (floc number). The cumulative distribution showed in the histograms (i.e., red line and squares Figures 6–9) presents some disadvantages for comparing flocs size distribution and flocs number of different water samples given the following reasons. First, the cumulative distributions tend to hide important aspect to the data. Second, the x-axis is highly depended on the lower limit of detection. Third, the use of an arithmetic scale to measure particle size (either diameter or volume) tends to compress the data for small sizes and spread out the data for the larger sizes (Chakraborti *et al.* 2000; Benjamin & Laurer 2013). To overcome this problem when comparing the different floc size distribution and number of flocs found in a water sample, it is recommended to plot the floc size diameter against a floc number distribution using a logarithmic scale (Chakraborti *et al.* 2000; Bache & Rassol 2001). Figure 11 shows the floc number distribution plotted as a function of the particle size for all four waters tested using a logarithmic scale. Figure 11 shows that for all waters tested, a similar floc size distribution was obtained and that the only significant difference among them was the number of flocs (y-axes).

The number of flocs for the different waters tested from the highest to the lowest was $\text{VQ} > \text{BB} > \text{SR} > \text{TM}$. The highest floc number concentration found in VQ water had two different peaks, the first at 85 μm and the second at 170 μm . These peaks indicate that a high percentage of the flocs have a size between 85 and 170 μm . The second water with a high concentration of flocs corresponds to BB water. This result is unexpected given its low raw water turbidity (i.e., 1.67 ± 0.11 NTU). This may suggest that the lack of particles in BB water does not allow to create large flocs and that a good quantity of fine flocs was created as a result of particle charge neutralization with a coagulant dose of 40 mg/L as Al_2O_3 . This statement was confirmed by the lowest mean floc area and perimeter found in BB water, i.e., 33,500 μm^2 and 710 μm , respectively (Figure 10). In addition, the lower floc number concentration found in SR water in comparison with VQ water could be the result of particle sweep coagulation removal being a predominant mechanism (Amirtharajah & Mills' 1989). The sweep coagulation promotes the formation of bigger and denser flocs (100–220 μm) instead of a high number of small flocs (<90 μm). This observation was confirmed by the larger mean area (104,471 μm^2) and perimeter (1,204 μm) of the flocs in SR water in comparison with the mean area (40,062 μm^2) and perimeter (745 μm) of the flocs in VQ water (Figure 10). Thus, measuring the floc perimeter and floc area is important to understand floc/particle destabilization and removal mechanisms and to design water treatment clarification units. Other methods such as the floc/particle's zeta potential analysis could be used to assess different floc/particle destabilization and removal

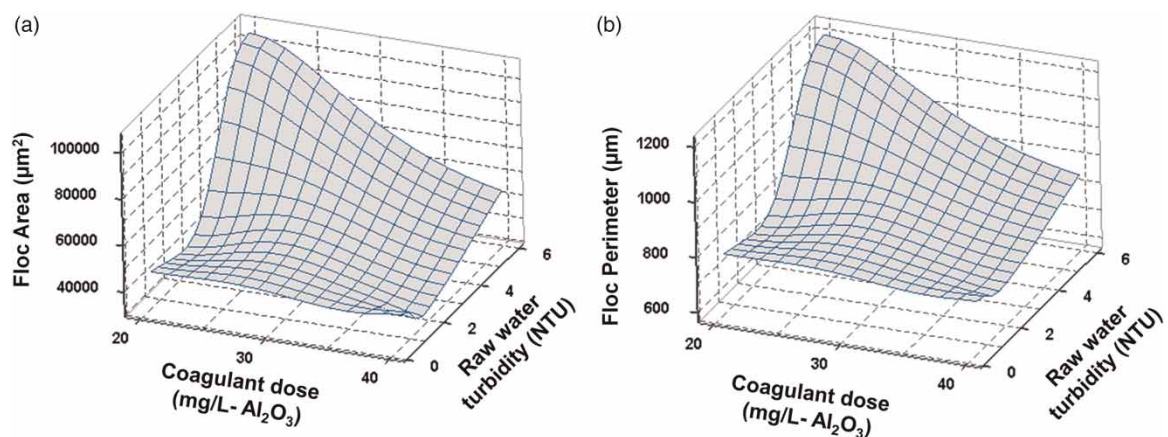


Figure 10 | Effect of raw water turbidity and coagulant dose on the flocs of the studied waters: (a) effect on floc surface area, and (b) effect on floc perimeter.

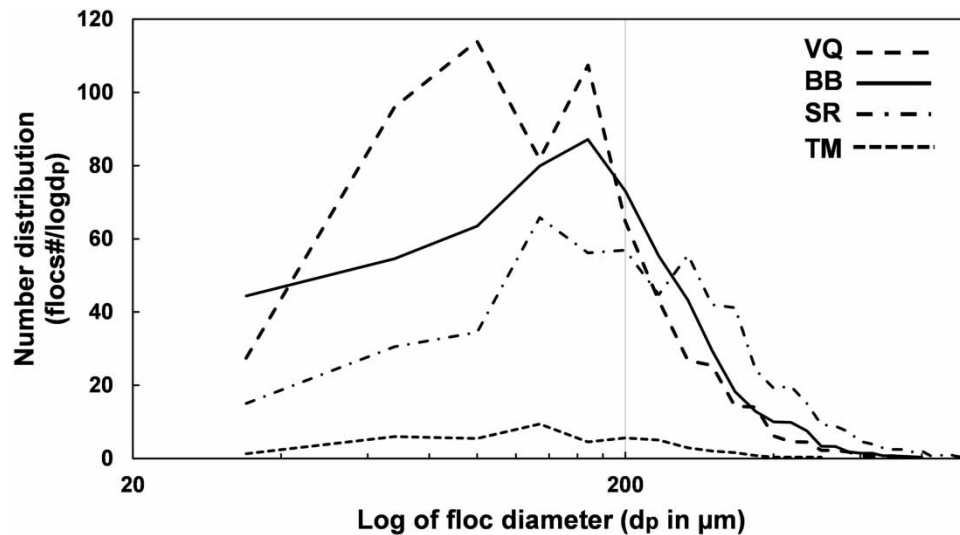


Figure 11 | Floc number distribution plotted as a function of the particle size for all waters tested.

mechanisms (Naceradska *et al.* 2019). However, in many cases the equipment for such analysis is not affordable for developing countries. The lowest floc concentration of all waters tested was found in TM water (Figure 11). This result agrees with its very low raw water turbidity (i.e., 0.53 ± 0.02 NTU). Furthermore, for this water the optimum alum coagulant dose (i.e., 40 mg/L as Al_2O_3) did not have a significant impact on the number of flocs, area, and perimeter (Figure 10).

Mean floc size variability as a function of the total flocs measured in a water sample

Figure 12 assesses the mean floc size variability as a function of the flocs number measured for a single picture containing approximately 1,300 flocs (blank diamond markers) and five pictures with a total of 5,500 flocs for BB, VQ and SR water and 1,964 flocs for TM water (black diamond markers). Given the broad range of floc sizes in both cases, the confidence limits of the mean floc size overlap. Thus, the mean size flocs for both cases are statistically the same (Figure 12). Therefore, it is possible to conclude that for assessing the mean floc size in a sample of water, measuring just one picture is sufficient to achieve an acceptable floc size characterization (i.e., mean floc size, floc size distribution, floc area, and floc perimeter).

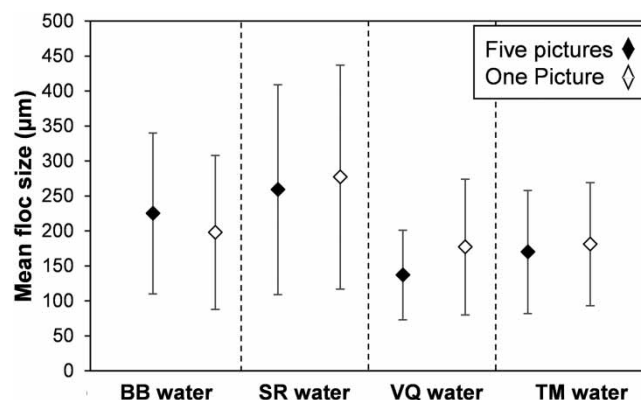


Figure 12 | Mean floc size obtained with one picture versus five different pictures (error bars indicate standard deviation) ($n=1300$) for one picture in each water except for TM water ($n=100$) and for five pictures ($n=5500$) in each water except for TM water ($n=1964$).

CONCLUSIONS

A low-cost nonintrusive method for floc size characterization has been developed and tested with four different surface waters using a regular HUAWEI P30 cell phone camera and a free computer program. The method showed to be useful to identify and measure flocs ranging in size between $33 \mu\text{m}$ and $1,200 \mu\text{m}$. This range of

flocs is consistent with the floc sizes reported by other researchers who used more complex imagery analysis techniques for alum floc characterization with size of (10–400 μm). In addition, a wide range of floc size distribution was possible to obtain for the different waters tested. Important physical floc characteristics such as area, perimeter, and shape factor were also obtained with the proposed methodology. The floc size characterization technique used in this study should be employed with surface waters having a maximum raw water turbidity of 6.0 NTU. Waters with the highest turbidity may not allow single flocs to be identified and measured as many flocs/particles within the jar make visualization and processing difficult by the computer program. For those cases, other techniques must be used. The proposed methodology could be useful for water treatment operators and managers in developing countries, specifically to optimize and control coagulation and flocculation process and to design and optimize direct filtration units to treat low turbidity and low alkalinity waters.

ACKNOWLEDGEMENTS

This research was supported by the Universidad Santo Tomás Colombia. The authors would like to thank the operators and managements of Boyacá, Soracá, Ventaquemada, and Turmeque in Boyacá Colombia for providing water samples, and plant information.

CONFLICT OF INTEREST

The authors declare no competing financial interest.

DATA AVAILABILITY STATEMENT

All relevant data are included in the paper or its Supplementary Information.

REFERENCES

- Aguilar, M. I., Saez, J., Llorens, M., Soler, A. & Ortuno, J. F. 2003 [Microscopic observation of particle reduction in slaughterhouse wastewater by coagulation flocculation using ferric sulphate as coagulant and different coagulant aids](#). *Water Research* **37**, 2233–2241.
- Amirtharajah, A. & Mills, K. M. 1989 [Rapid-mix design for mechanisms of alum coagulation](#). *Journal of New England Water Works Association* **74**(4), 210–216.
- APHA/AWWA/WEF 2017 *Standard Methods for the Examination of Water and Wastewater*, 23th edn. American Public Health Association/American Water Works Association/Water Environment Federation, Washington, DC, USA.
- AWWA 2011 *Manual M37—Operational Control of Coagulation and Filtration Processes*. American Water Works Association, Denver, CO.
- Bache, D. H. & Rassol, E. 2001 [Characteristics of alumino-humic flocs in relation to DAF performance](#). *Water Science and Technology* **43**, 203–208.
- Benjamin, M. M. & Laurer, D. F. 2013 *Water Quality Engineering Physical/Chemical Treatment Processes*. John Wiley & Sons, New Jersey, New York, USA.
- Chakraborti, R. J., Atkinson, J. F. & Van Benschoten, J. E. 2000 [Characterisation of alum floc by image analysis](#). *Environmental Science and Technology* **34**, 3969–3976.
- Constantine, T. A. 1982 [Advanced water treatment for color and organics removal](#). *Journal of the American Water Works Association* **74**, 310–313.
- Dastanaie, A. J., Bidhendi, G. R., Nasrabadi, T., Habibi, R. & Hoveidi, H. 2007 [Use of horizontal flow roughing filtration in drinking water treatment](#). *International Journal of Environmental Science and Technology* **4**(3), 379–382.
- Dempsey, B. B. & O'Melia, C. R. 1984 [Removal of naturally occurring compounds by coagulation and sedimentation](#). *Critical Reviews in Environmental Control* **14**(4), 311–331.
- Edzwald, J. K. 2010 [Dissolved air flotation and me](#). *Water Research* **44**, 2077–2106.
- Edzwald, J. K. & Haarhoff, J. 2012 *Dissolved air Flotation for Water Clarification*. American Water Works Association and McGraw-Hill, Inc, New York, USA.
- El-Taweel, G. E. & Gamila, H. A. 1999 [Evaluation of roughing and slow sand filters for water treatment](#). *Water, Air, and Soil Pollution* **120**, 21–28.
- Feride, U., Erhan, G. & Mehmet, K. 2019 Removal of natural organic matter from Lake Terkos by EC process: studying on removal mechanism by floc size and zeta potential measurement and characterization by HPSEC method. *Water Process Engineering* **31**(10), 100831.
- González-Galvis, J. P. & Narbaitz, R. M. 2020a Large batch bench-scale dissolved air flotation system (LB-DAF) for drinking water treatability tests. *Environmental Science: Water Research & Technology* **6**, 1004–1017.
- González-Galvis, J. P. & Narbaitz, R. M. 2020b Large batch bench-scale dissolved air flotation system for simulating full-scale turbidity removal. *Environmental Technology*, ed: Taylor & Francis, 0–14.

- Gorczyca, B. & Ganczarczyk, J. 1999 Structure and porosity of alum coagulation flocs. *Water Quality Research Journal of Canada* **34**, 653–666.
- Goula, A. M., Kostoglou, M., Karapantsios, T. D. & Zouboulis, A. I. 2008 The effect of influent temperature variations in a sedimentation tank for potable water treatment— a computational fluid dynamics study. *Water Research* **42**, 3405–3414.
- Gregory, J. 1998 Turbidity and beyond. *Filtration & Separation* **35**(1), 63–67.
- Hoyos, N., Escobar, J., Restrepo, J. C., Arango, A. M. & Ortiz, J. C. 2013 Impact of the 2010–2011 La Niña phenomenon in Colombia, South America: the human toll of an extreme weather event. *Applied Geography* **39**, 16–25.
- Hunsinger, R. B., Roberts, K. J. & Lawrence, J. 1980 Chrysolite asbestos fiber removal during potable water treatment. Pilot plant studies. *Environmental Science & Technology* **14**(3), 333.
- INS 2019 Estado de la Vigilancia de la Calidad del Agua para Consumo Humano en Colombia (SIVICAP). Bogotá D.C., Colombia. Available from: http://aplicacionespruebas.ins.gov.co/sivicap_new/Reports/IrcaByDepartment/ (May 2020).
- Jarvis, P., Jefferson, B. & Parsons, S. A. 2006 Floc structural characteristics using conventional coagulation for a high doc, low alkalinity surface water source. *Water Research* **40**, 2727–2737.
- Juntunen, P., Liukkonen, M., Lehtola, M. & Hiltunen, Y. 2014 Characterization of alum flocs by image analysis in water treatment processes. *Cogent Engineering* **1**, 1–13.
- Kavanaugh, M. C., Tate, C. H., Trussel, A. R. & Treweek, G. 1980 Use of particle size distribution measurements for selection and control of solid liquid separation processes. Particulates in water, Eds. American Chemical Society, Washinton D.C. chap. 14.
- Kawamura, S. 2000 *Integrated Design and Operation of Water Treatment Facilities*, 2nd edn. Wiley-Interscience, New York, USA.
- Lawrence, J. & Zimmermann, H. W. 1976 Potable water treatment for some asbestiform minerals: optimization and turbidity data. *Water Research* **10**, 195.
- McCurdy, K., Carlson, K. & Gregory, D. 2004 Floc morphology and cyclic shearing recovery: comparison of alum and polyaluminium chloride coagulants. *Water Research* **38**, 486–494.
- Mesa, O., Poveda, G. & Carvajal, L. 1997 *Introducción al clima de Colombia*. Universidad Nacional de Colombia, Bogotá.
- Movrocordatos, D., Stainer, M. & Boller, M. 2004 Analysis of environmental particles by atomic force microscopy, scanning and transmission electron microscopy. *Water Science and Technology* **50**(12), 9–18.
- MWH 2012 *Water Treatment: Principles and Design*, 2nd edn. John Wiley & Sons, New Jersey, New York, USA.
- Naceradska, J., Pivokonska, L. & Pivokonsky, M. 2019 On the importance of pH value in coagulation. *Water Supply Research and Technology AQUA* **68**(3), 222–230.
- Poveda, G. & Mesa, O. 1996 Las fases extremas del ENSO e El Niño y la Niña e y su influencia sobre la hidrología de Colombia. *Revista Ingeniería Hidráulica* **11**(1), 21–37.
- Poveda, G., Jaramillo, A., Gil, M., Quiceno, N. & Mantilla, R. 2001 Seasonality in ENSO-related precipitation, river discharges, soil moisture, and vegetation index in Colombia. *Water Resources Research* **37**(8), 2169–2178.
- Sillanpää, M., Ncibi, M. C., Matilainen, A. & Vepsäläinen, M. 2018 Removal of natural organic matter in drinking water treatment by coagulation: a comprehensive review. *Chemosphere* **190**, 54–71.
- Sun, S., Weber-Shirk, M. & Lion, L. W. 2016 Characterization of flocs and floc size distribution using image analysis. *Environmental Engineering Science* **33**(1), 25–34.
- Wang, X. C. & Gregory, J. 2002 Structure of Al-Humic flocs and their removal at slightly acidic and neutral pH. *Water Science and Technology* **2**(2), 99–106.
- Wang, Z., Teychene, B. & Abbott Chalew, T. E. 2014 Aluminum-humic colloid formation during pre-coagulation for membrane water treatment: mechanisms and impacts. *Water Research* **61**, 171–180.
- Zafisah, N. S., Ang, W. L., Mohammad, A. W. & Hilal, N. 2020 Interaction between ballasting agent and flocs in ballasted flocculation for the removal of suspended solids in water. *Water Process Engineering* **33**, 101–028.

First received 26 October 2021; accepted in revised form 15 March 2022. Available online 25 March 2022